Brain Tumor Detection of Skull Stripped MR Images Utilizing Clustering and Region Growing

S.M. Ali[1], Loay K. Abood [2], Rabab S. Abdoon[1*]
[1] Remote Sensing Research Unit, College of science, University of Baghdad, Baghdad, Iraq.
[2] Department of Computer Science, College of science, University of Baghdad, Baghdad, Iraq .

Abstract

Brain tissues segmentation is usually concerned with the delineation of three types of brain matters Grey Matter (GM), White Matter (WM) and Cerebrospinal Fluid (CSF). Because most brain structures are anatomically defined by boundaries of these tissue classes, accurate segmentation of brain tissues into one of these categories is an important step in quantitative morphological study of the brain. As well as the abnormalities regions like tumors are needed to be delineated. The extra-cortical voxels in MR brain images are often removed in order to facilitate accurate analysis of cortical structures. Brain extraction is necessary to avoid the misclassifications of surrounding tissues, skull and scalp as WM, GM or tumor when implementing segmentation algorithms. In this work, two techniques have been implemented to extract the brain tissues as elementary step. The next step was utilizing the resultant skull stripped images as input of four segmentation algorithms to extract the tumor region and calculate the area value of it. The resultant skull stripped images for complete set of T2-weighted images and the adaptive K-Means clustering techniques proved the robust performance of these proposed algorithms.

Keywords*:* Brain Tumor, Active Contour, Clustering, Region Growing, Morphological Operations, MRI.

الكشف عن أورام الدماغ في صور الرنين المغناطيسي منزوعة الجمجمة بأستخدام طرق العنقدة وانماء المناطق

صالح مهدي علي[1] ، لؤي كاظم عبود[2] ، رباب سعدون عبدون*[1]
[1]وحدة الاستشعار عن بعد، كلية العلوم، جامعة بغداد ، [2] قسم الحاسبات ، كلية العلوم، جامعة بغداد ، بغداد، العراق

الخلاصة

ان عملية تقسيم الانسجة الدماغية تنطوي على تحديد ثلاثة انواع من المادة الدماغية وهي ا لمادة الرمادية والمادة البيضاء والسائل الشوكي . ولكون معظم تراكيب الدماغ تعرف تشريحيا من خلال حدود هذه الانسجة لذا فان التقسيم الدقيق لانسجة الدماغ الى واحدة من هذه الاصناف تعتبر خطوة مهمه في الدراسة الطوبوغرافية النوعية لانسجة الدماغ . كما وان المناطق الغير طبيعية مثل الاورام تحتاج ايضا الى تحديد. ان الفوكسلات العائدة لمناطق خارج المخ في صور الرنين المغناطيسي للدماغ تزال عادة لتسهيل عملية التحليل الدقيق للتراكيب اللحائية. ان عملية استخلاص النسيج الدماغي هي عملية ضرورية لتجنب سوء التصنيف للانسجة المحيطة مثل الجمجمة والفروة على انها مادة بيضاء او مادة رمادية أو ورم عند تطبيق خوارزميات التقسيم . في هذا العمل تم تطبيق تقنيتين لغرض استخلاص النسيج الدماغي كخطوة ابتدائية . والخطوة التالية استخدام

*Email:sr614@ymail.com

الصورة الناتجة المنزوعة الجمجمة كمدخلات لاربعة من خوارزميات التقسيم لاستخلاص منطقة الورم ومن ثم حساب قيمة المساحة له. ان الصور المنزوعة الجمجمة الناتجة لمجموعة كاملة من صور T2 المرجحة وتقنية عنقدة وسائل الـk المطورة قد اثبتت الاداء المحكم لهذه التقنيات المقترحة.

Introduction

Segmentation subdivides an image into its constituent regions or objects [1]. Image segmentation is one of the most difficult tasks in image processing; its accuracy determines the eventual success or failure of computerized analysis procedures. Consequently, considerable care have been taken to improve the probability of accurate segmentation [2]. Segmentation techniques can be classified into; classical techniques such as thresholding, boundary based technique, region based technique, or statistical based technique. Depending on the level of interactivity, segmentation can be classified as manual, semi-automatic or automatic [3, 4]. Despite numerous efforts and promising results achieved in the medical imaging field, accurate segmentation and isolation of abnormalities is still a challenging and difficult mission because the overlapping existed between brain's tissues, and the variety in the shapes, locations and image intensities of abnormalities [5]. In this work, skull stripping process has been implemented to extract the brain tissues without any extra-cortical parts. Two techniques have been adopted to accomplish this task: successive morphological operations and deformable model (active contour). The resultant skull stripped image has been smoothed using bilateral filter to reduce the staircase effects among image points. Many segmentation techniques have been utilized, some of them were adapted methods; e.g. K-Means based on K-Means, Fuzzy C-Means, K-Means based on Fuzzy C-Means and Region Growing.

Skull Stripping

The skull-stripping aims to extract the brain from the skull, eliminating all non-brain tissues (e.g. bones, scalp, fat, veins, eyes, skin, and meningitis). This procedure requires a semi-global and local understanding of the skull and brain image, imaging artifacts, anatomical variability, and varying contrast properties [6]. The extra-cortical voxels (volume element) in MR brain images are often removed in order to facilitate accurate analysis of cortical structures i.e. to avoid the misclassifications of surrounding tissues, skin and scalp as WM or GM [7]. Generally, skull stripping methods are classified into three types: intensity based, morphology based and deformable model based. The extraction of the brain region from the non-brain region can be performed by methods like region growing, watershed and mathematical morphological methods [6].In this work, two different techniques have been suggested and implemented to achieve this task; i.e. successive morphological operations and active contour algorithm.

Morphological Operations

Morphological operators have been used for their vigorous performance in preserving the shape of a signal, while suppressing the noise [8]. Image morphology provides a way to incorporate neighborhood and distance information into algorithms. There are two basic morphological operators: *Erosion* and *Dilation* or *Opening* and *Closing* which were derived from the erosion and dilation. Number of pixels added or removed from an object in an image depends on the size and shape of the structuring element used to process the image [9]. These operations have been applied successfully to a broad variety of image processing analysis tasks, for more details see [10-13]. In this study, *Disk-shape* template form is utilized since the brains possess approximate oval shape.

Deformable Models

The deformable models (also known as ***active contours*** or/and ***snakes***) are often used to approximate the locations and shapes of object boundaries in images based on the reasonable assumption; i.e. the boundaries that are piecewise continuous or smooth in an image which can be moved due to the influence of internal and external forces [14]. The active contour models lock onto nearby edges, localizing them accurately; they can be used to fit the object's shape by minimizing a gradient dependent attraction force while at the same time maintaining the smoothness of the contour shape, [15]. Thus, unlike edge detection, active contour methods are much more robust, in case of

image noise existence, as the requirements for contour smoothness, and contour continuity was required. Another advantage of this model is that; prior knowledge about the shape of the object can be built into the contour parameterization process. Active contour methods have difficulty in handling deeply convoluted boundaries (e.g. CSF, GM and WM boundaries), due to their contour smoothness requirement. Hence, they are often inappropriate for the segmentation of brain tissues. Nevertheless, they have successfully applied to the segmentation of intracranial boundary [16], brain outer surface [17], and neuro-anatomic structures in MR brain images [18].

The active contour is represented by a vector, *v*, which contains all of the *n* points of the snake. The functional energy of this snake is given by [19]:

$$E = \int \left[E_{\text{int}} \left(v(s)\right) + E_{image} \quad (v(s)) \right] ds$$
$$= \int \left| \alpha(s) E_{cont} \left(v(s)\right) + \beta(s) E_{curv} \quad + \gamma(s) E_{image} (v(s)) \right| ds \qquad (1)$$

Where: E_{int} is the internal energy of the contour, it consists continuity energy E_{cont} plus curvature energy E_{curv}. E_{image} represents the proper energy of the image, which is very different from one image to another. $\alpha, \beta, and\ \gamma$ are values that can be chosen to control the influence of the three terms [20-21].

K -Means Clustering Algorithm

Among the hard clustering methods, K-means is an extensively used clustering algorithm to partition data into certain number of clusters [22]. It is an iterative technique that is used to partition an image into 'k' clusters, the process involves of grouping data points with similar feature vectors into a single cluster and grouping data points with dissimilar feature vectors into different clusters [23].

Fuzzy C-Means Clustering Algorithm

Fuzzy C-Means (FCM) algorithm is the most popular method used in image segmentation because it has robust characteristics for ambiguity and can retain much more information than hard segmentation methods [24]. Conventional and modified FCM algorithm has been widely studied and successfully applied in medical image segmentation by many researchers. The conventional FCM algorithm is efficiently used for clustering in medical MRI brain images because the uncertainty of MRI image is widely presented in data, in particular, the transitional regions between tissues are not clearly defined and their memberships are intrinsically vague [25]. In FCM algorithm the data patterns may belong to several clusters, having different membership values with different clusters. The membership value of a data to a cluster denotes similarity between the given data pattern to the cluster see [26].

Region Growing Algorithm

Region growing methods usually start by locating some seeds representing distinct regions in the image [27-28]. The seeds are then grown until they eventually cover the entire image. The region growing process is therefore governed by a rule that describe the growth mechanism and a rule that check the homogeneity of the regions at each growth step [29]. This algorithm begins with selecting ***n*** seed pixels, each seed pixel "***i"*** is treated as a region A_i , $i \in \{1, 2 \ldots n\}$. The algorithm then try to find some neighboring pixels to those regions and merging them with the original regions that having similar intensities. The choice of homogeneity criterion is crucial for the success of this algorithm, for example the homogeneity criterion proposed in [28, 30] is the difference between the pixel intensity value and the mean intensity value of the region: i.e.

$$\delta(x) = |g(x) - mean[g(y)]|, \quad y \in A_i \qquad (2)$$

Where: $g(x)$ is the gray value of the image point *x*, and x is an unallocated pixel which is adjacent to region A_i.

Adaptive K-Means / K-Means based on FCM and K-Means based on K-Means

It is well known that the output of K-Means algorithm depends hardly on the initial seeds number as well as the final cluster numbers. Therefore to avoid such obstacle, K-Means based on FCM is suggested in our previous paper [31]. The idea behind that suggestion was to supply the K-Means with well-defined clusters centers based on optimal calculation instead of random ones. In addition, the FCM algorithm assign probability for each pixel to be classified rather than deterministic class assignment by K-Means, so one can switch from probability to deterministic by this algorithm. Moreover, an adaptive technique is suggested here which based on the centers of K-Means clustering that is implemented on abnormal image belongs to the same dataset under study.

Experimental Dataset, Methodologies and Results

The experimental dataset that utilized in this work has been obtained from the Whole Brain Atlas website of patient with a malignant tumor. The adopted set was T2-weighted MRI modality of 22 images (named U1T2-U22T2). Figure 1- presents samples of these images.

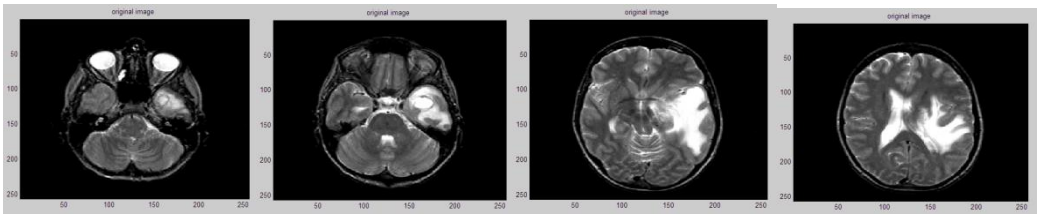

Figure 1- Samples of the experimental images

Skull stripping utilizing Morphological Operations

In this part of the work, many morphological operations have been implemented to extract the brain tissues of the complete sets (U1T2-U22T2) images presented in the first column of fig.(4); these operations are:

i. Binarizing the images by utilizing a suitable thresholding value depending on the image gray levels (the value *50* is adopted for most of them).

ii. Applying morphological opening process with structuring element of disk-shape of radius equals *seven* pixels.

iii. Selecting the maximum area (area that exceeds a specific number of pixels) this number depending on the slice position, (it is ranged from 350-760 pixels).

iv. Applying morphological closing process with structuring element of disk-shape of radius equals *seven* pixels. After that filling holes if they presents.

v. Multiplying the resultant image by the input image to obtain grey level image of the extracted brain tissues.

The main steps of implementing this technique on one image are illustrated in fig.(2),while the results of implementing this technique on the complete dataset images are illustrated in the second column of figure 2-.

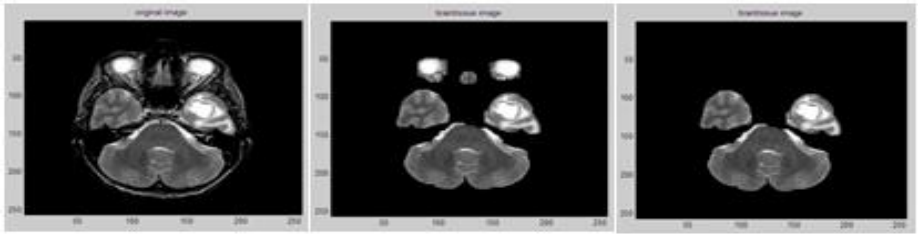

Figure 2- The resultant images of the skull stripping algorithm using morphological operations. First image, input image, the second one, output image after applying morphological operations, and the third one, final brain tissue after selecting the maximum area.

Skull Stripping utilizing Active Contour Algorithm

In this part of the work, skull stripping process has been applied by implementing active contour algorithm on the complete set (U1T2-U22T2).This process has been implemented with initialization element of circle-shape with suitable radius. The radii of the initialization element were ranged from (20-70) pixels within the brain region. The size and position of initialization element depending on the slice's shape and location within the head. This algorithm is applied with maximum number of iterations equals 1250 and the value of alpha parameter equals 0.2.

The steps of implementing this technique on two images are illustrated in figure 3-, while the results of implementing this technique on the complete set images are presented in the third column of figure 4-.

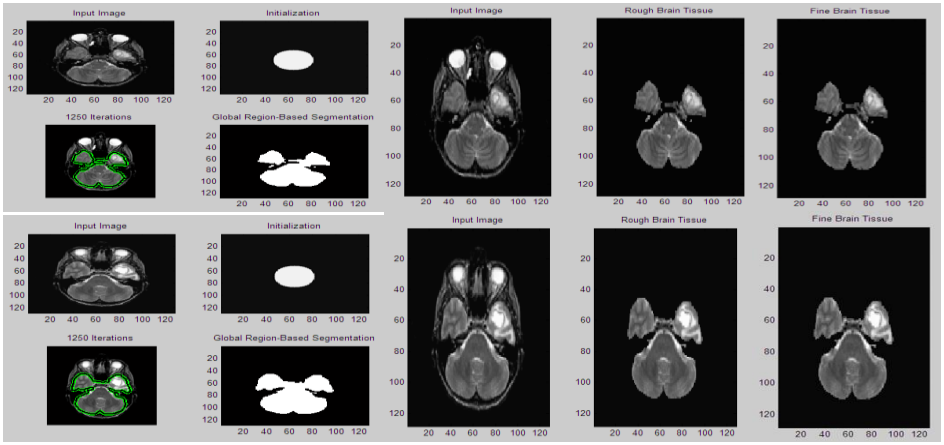

Figure 3- Shows the steps of the skull stripping process using active contour for two input images with initialization element of circle within the brain tissue region.

K-Means Clustering Algorithm based on K-Means Centers

To unify the classes of the different tissues of the brain of the all abnormal images K-Means algorithm was applying on one abnormal image and then adopting the values of the clusters' centers to pass them to the K-Means algorithm that implemented on the all slices' images later to get clustered images with the same clusters labels. This procedure has been done in steps as follows:

1-To get the cluster that the tumor belongs to, in the abnormal images (U3T2-U15T2), the K-Means algorithm has been implemented on image U8T2 after skull stripping and bilateral smoothing.

2- The centers values of the clusters of U8T2 segmented image has been passed to the K-Means algorithm that implemented later on the images (U3T2-U15T2) after skull stripping and bilateral smoothing too. The results of these steps are shown in the figures 5- and 6- for three images as samples.

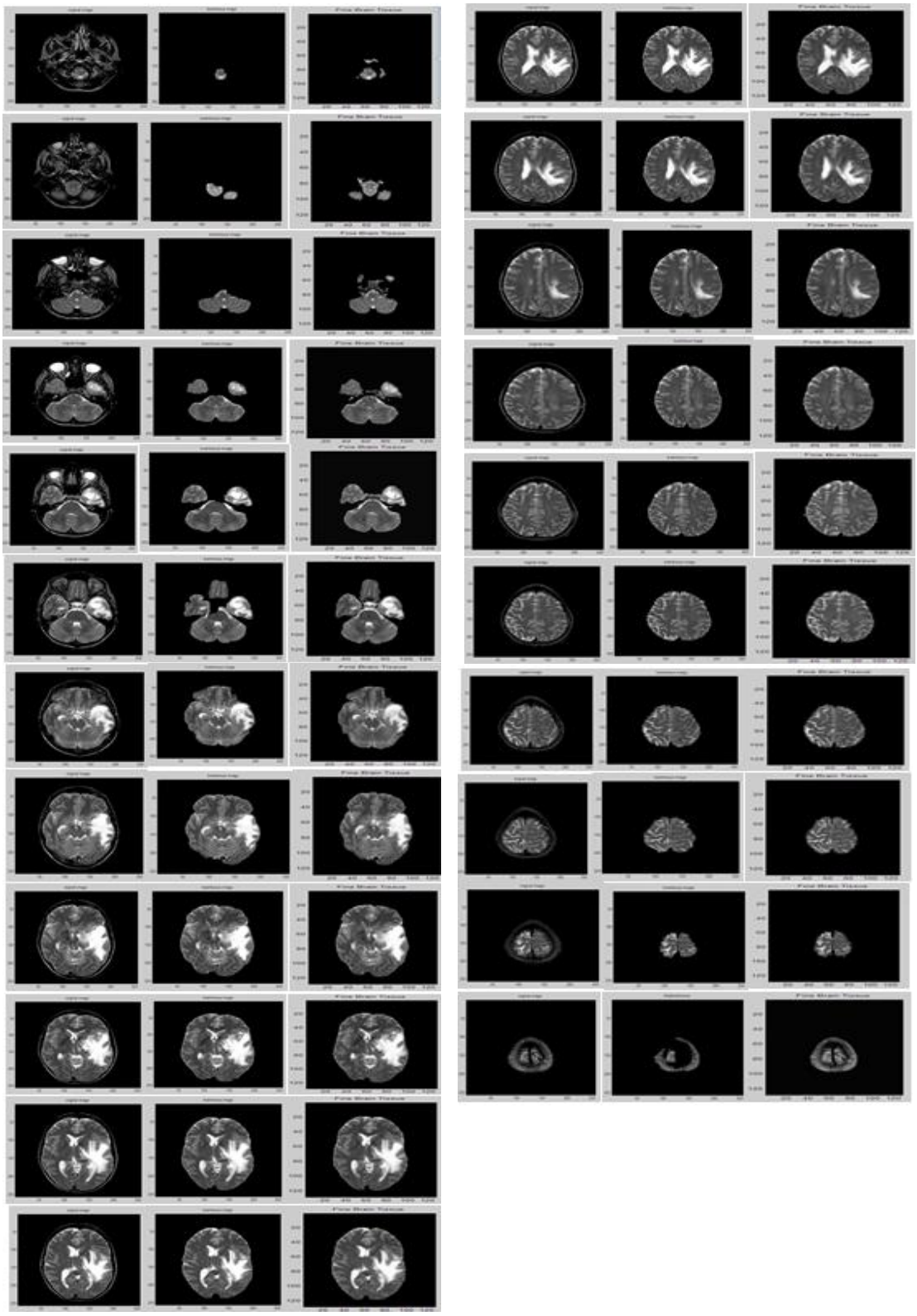

Figure 4- Shows the skull stripping process's results for the complete dataset. First column, the original image, the second column, the extracted brain tissue by applying morphological operations, and the third column, the extracted brain tissues by applying active contour algorithm.

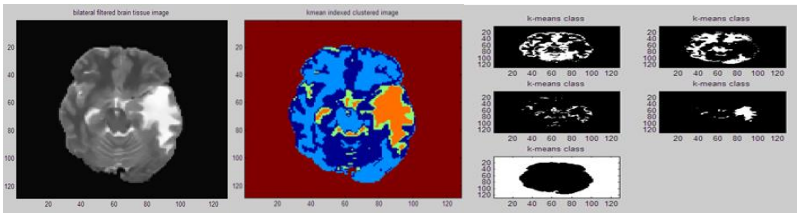

Figure 5- Shows the results of applying K-Means algorithm on U8T2 image. From left to right: first image, the extracted brain tissue image after bilateral filtering; second image, the segmented image; and last one, the clusters separately. It is obviously that, the cluster of the tumor is the fourth one.

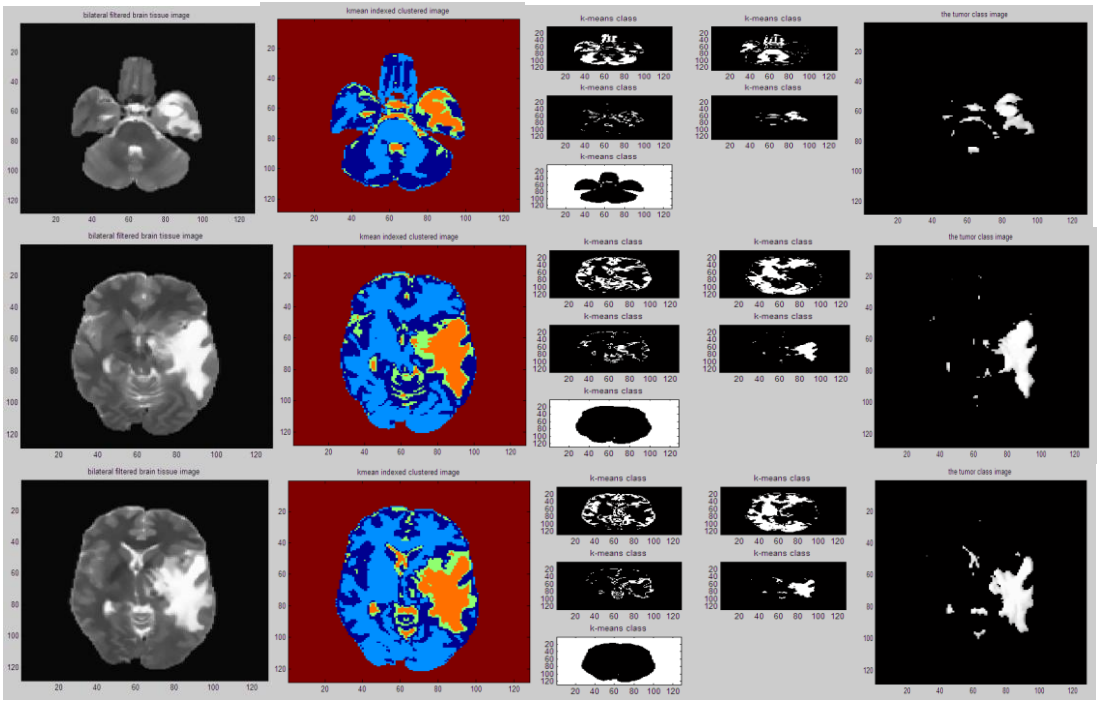

Figure 6- Shows the results of applying K-Means algorithm on three images as samples. First column, the brain tissue image after bilateral filtering; second column, the segmented image; third column, the clusters separately, and last column, the cluster of the tumor.

Fuzzy C-Means Clustering Algorithm

Fuzzy C-Means clustering algorithm has been implemented on the images (U3T2-U15T2) after skull stripping and bilateral filter smoothing processes. These images have been clustered into five clusters. The resultant segmented images, their five clusters, and the cluster that the tumor belongs to for four images as samples, are illustrated in figure 6-.

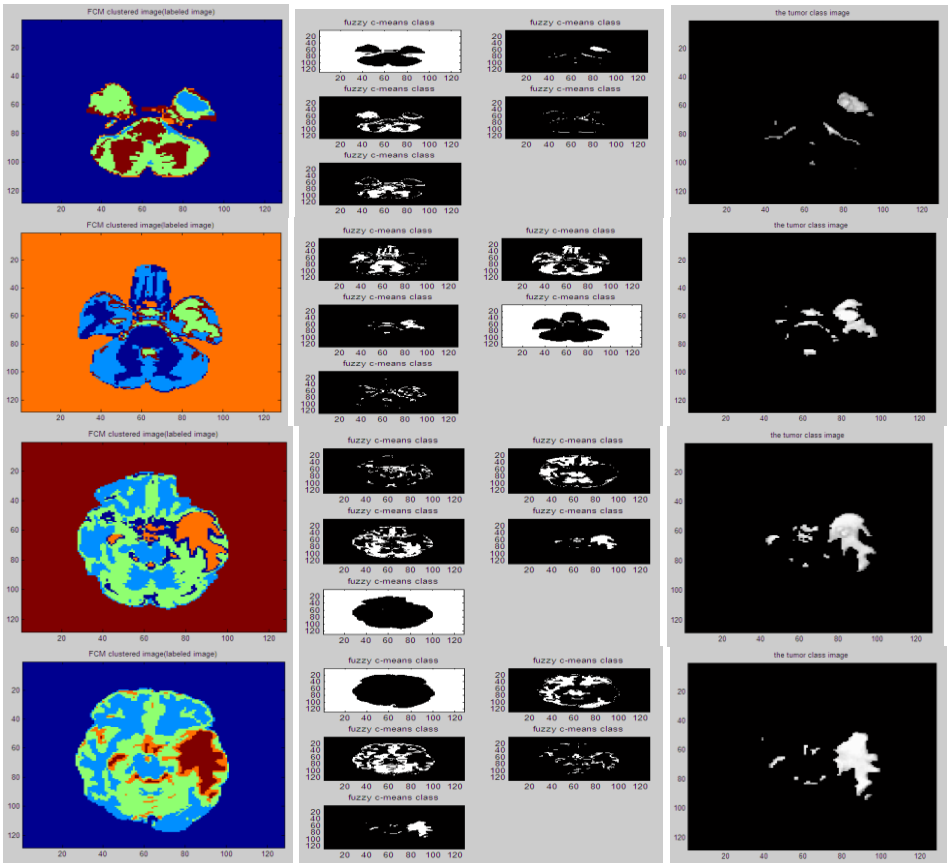

Figure 7- Shows the results of applying FCM clustering algorithm on the brain tissue images after bilateral filtering of four images. First column, the segmented image; second column, the clusters separately; and last column, the cluster of the tumor.

K-Means clustering Algorithm based on FCM

In this part of the work an adaptive technique has been implemented to segment the abnormal MR brain images. This technique is involved applying FCM clustering algorithm on one abnormal image, then passing the values of the centers of the clustered image to the K-Means algorithm that applied on the same image. After that, adopting the centers' values as centers' values of the K-Means algorithm to implement it later on the all abnormal slices' images. The procedure of this technique can be summarized as follows:

1. Implementing FCM algorithm on U8T2 image.
2. Pass the values of the centers of the clustered image to the K-Means algorithm that applied on the same image.
3. Pass these center values to the K-Means algorithm that implemented on the images (U3T2-U15T2).

The results of these steps are illustrated in the figures (8and 9) for four images as samples.

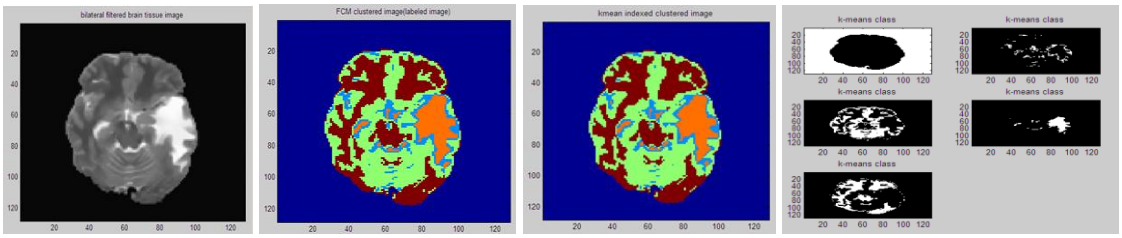

Figure 8- Shows the results of applying K-Means based on FCM on U8T2 image. From left to right: first image, the brain tissue after bilateral filtering; second one, FCM segmented image; third one, K-Means segmented image based on FCM; and last one, the clusters separately. It is obviously, the cluster of the tumor is the fourth one.

To compare of the performance of the three techniques: K-Means, FCM, and K-Means based on FCM clustering algorithms, two images U8T2 and U10T2 from the previous set, have been selected to extract the tumor regions that contained within them. The extraction process of the tumor regions from these images is illustrated in the figures (10 and 11) for the images U8T2 and U10T2 respectively.

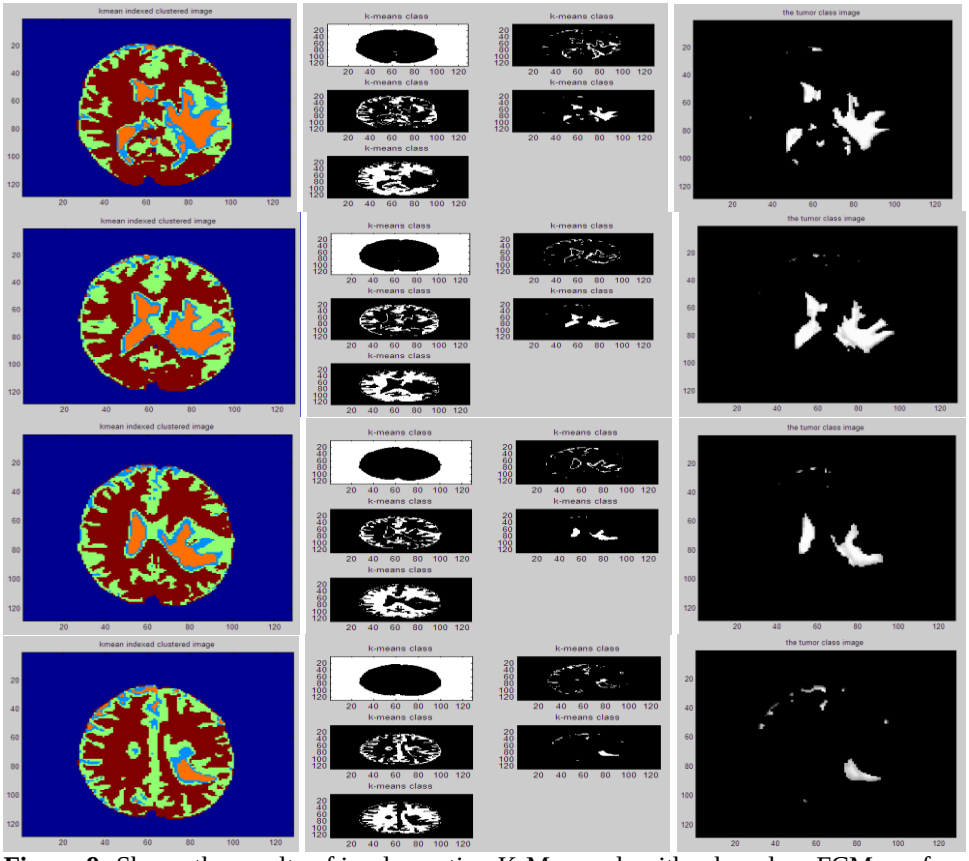

Figure 9- Shows the results of implementing K-Means algorithm based on FCM on four images. First column, the segmented image; second column, the clusters separately; and last column, the cluster of the tumor.

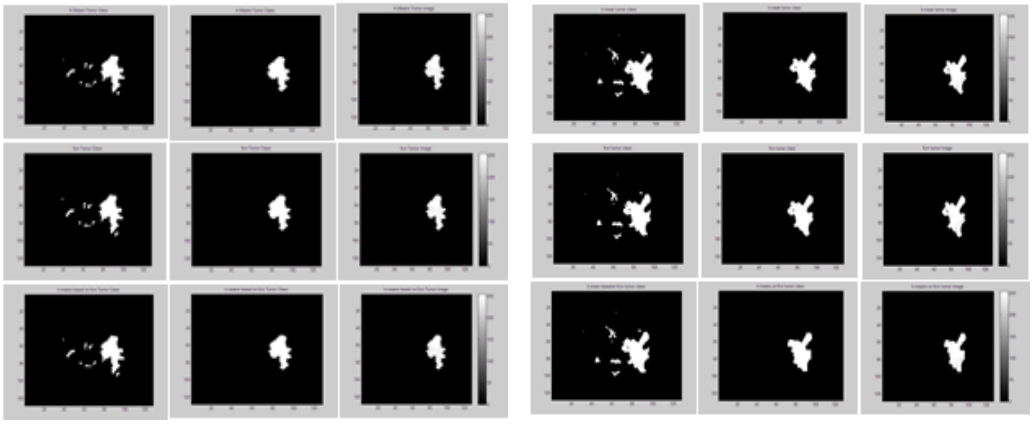

a b

Figure 10- Illustrates the steps of getting the tumor that extracted by implementing the algorithms:K-Means, FCM, and K-Means based on FCM from first row to the last one respectively. First column, the cluster of the tumor; second column, the tumor region class after morphological opening process; and third column, the grey level image of the tumor region (a) for image U8T2 and (b) for image U10T2.

First step is selecting the cluster that the tumor region belong to which are presented in the figures 10- (a & b) first column, after that, to extract the pixels of the tumor region only an opening morphological process has been applied with structuring element of disk-shape of radius equals *two* pixels for all the cases except the last one in figure 10 b-. The resultant images of this process are

presented in the second column, after that the gray level image of the tumor region is obtained by multiplying the tumor class image by the corresponding input image as illustrated in the third column.

The area of the extracted tumor regions that extracted from the previous procedure by implementing the algorithms: K-Means, FCM, and K-Means based on the centers' values of the FCM algorithm, are calculated and demonstrated in table 1- for the comparison.

Region Growing Segmentation Algorithm

In this part of the work the Region Growing segmentation algorithm has been implemented on the abnormal images (U3T2-U15T2). Firstly, the images have been skull stripped and then the bilateral filter has been applied. After that Region Growing segmentation algorithm has been implemented with thresholding value equals 25, and the resultant segmented images have been demonstrated in figure 11- for ten images as samples.

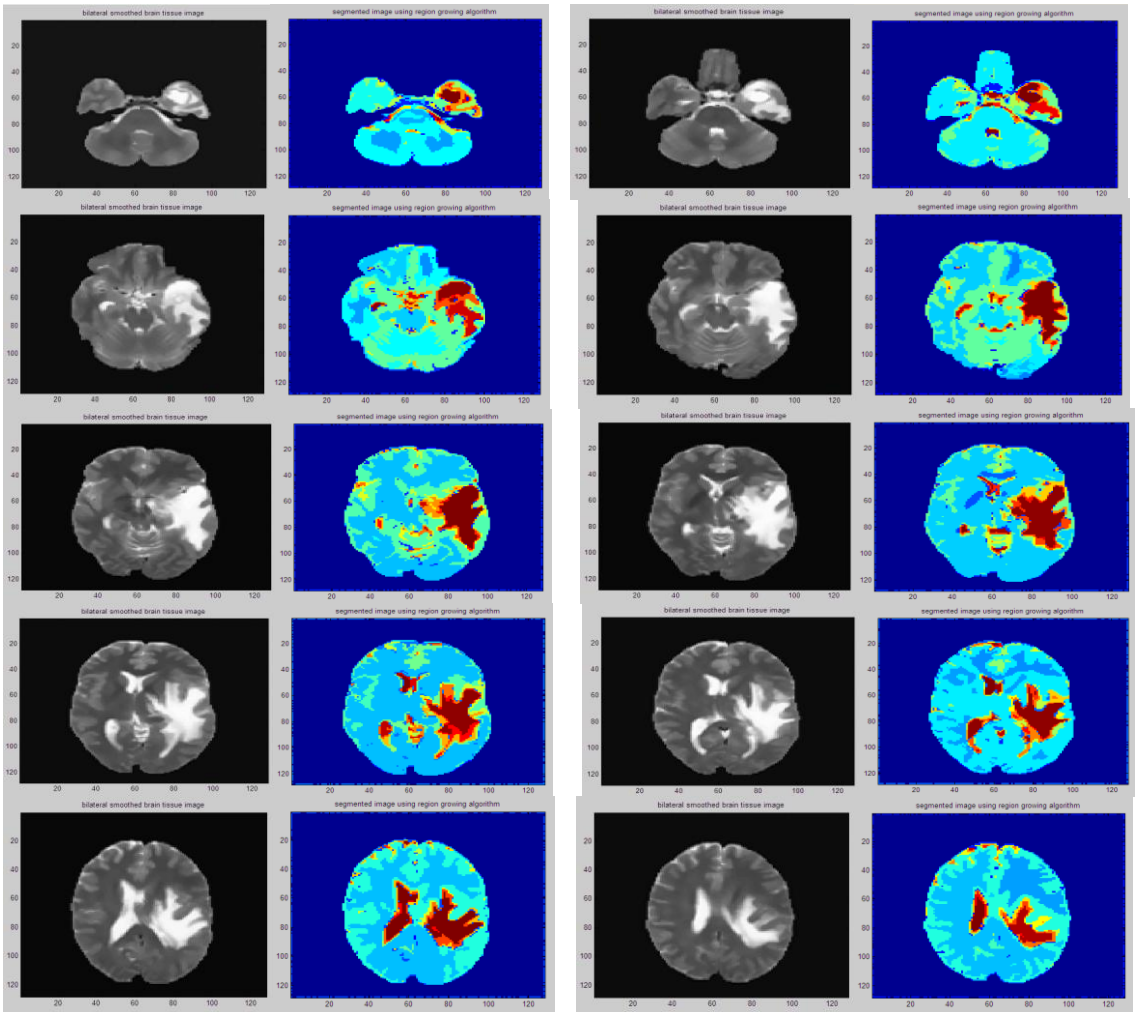

Figure 11- Shows the results of applying Region Growing algorithm on ten images. First image represents the brain tissue image after bilateral filtering, and the second image represents the output segmented image
(labels Broun & red indicate the abnormality regions).

Comparison of the Different Segmentation Algorithms

In this section a visual comparison of the segmented images that obtained by implementing different segmentation techniques, is presented. Figure 12- demonstrates the segmented images by implementing the algorithms: K-Means; K-Means based on FCM; FCM; and Region Growing. All these algorithms have been implemented on skull stripped and bilateral filtered images. Figure12- illustrates the results for four images as samples.

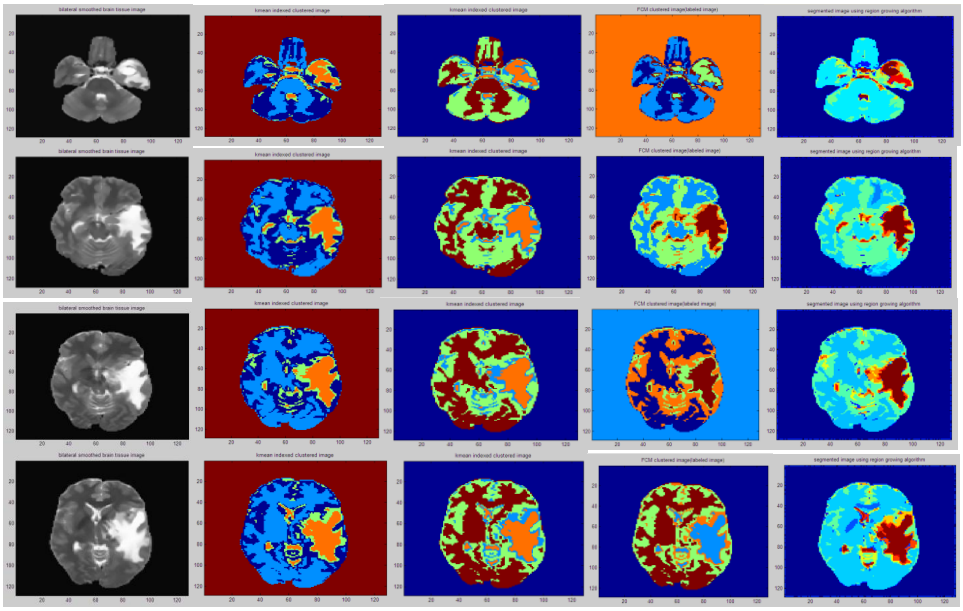

Figure 12- A comparison of results of different segmentation techniques for four abnormal images. First column, the brain tissue images after bilateral filtering. Second column, the segmented image using K-Means. Third column, the segmented image using K-Means based on FCM. Fourth column, the segmented image using FCM. The last column, the segmented image using Region Growing algorithm.

Table 1- Illustrates the area of the extracted tumor regions from the images U8T2 and U10T2, by implementing the algorithms: K-Means, FCM, and K-Means based on FCM algorithm.

Area (Pixels)	Image	Algorithm		
		K-Means	FCM	K-Means based on FCM
	U8T2	1920	1940	1940
	U10T2	2628	2660	2456

Conclusions

In this work, two techniques have been adopted to extract the brain tissues. These techniques are: many successive morphological operations and active contour algorithm. The results show high quality performance of these two techniques with superior of the active contour. These techniques succeeded for the complete set images except the last one. By inspection of the results of the proposed segmentation algorithms carefully: K-Means based on K-Means, FCM, K-Means based on FCM and region growing, one can deduce different points of view for the best performance. If the main goal is to detect the abnormality (tumor region); Region Growing will be the best; if the interest is the details of different regions, FCM is the best and so; i.e. each method has its own properties. Finally when the tumor region is the goal, so Region Growing is the best here, where the tumor is very distinct and clear. The important notice here is that the used threshold in Region Growing is (25); the property of such images (MRI) allow us to use such range of threshold where the tissue type in the brain image is limited. Therefore the final image is so soft, low fine details, and high accuracy of tumor resolving.

References

1. Gonzalez R.C. and Woods R.E. **2008**. *Digital Image Processing*. Prentice Hall, New Jersey.
2. Indah S., Adhi S., Thomas S. W. and Maesadji T. **2011**. Optimized Fuzzy Logic Application for MRI Brain Images Segmentation. *International Journal of Computer Science & Information Technology (IJCSIT)*. 3(5).
3. Tomi H., Prasun D., Harry F., Hannu E. **1999**. Applications of MR Image Segmentation. *International Journal of Bioelectromagnetism*, 1(1). pp: 35-46.
4. Jagath C. Rajapakse, Jay N. Giedd, and Judith L. R., **1997**. Statistical Approach to Segmentation of Single-Channel Cerebral MR Images. *IEEE Transactions on Medical Imaging*, 16(2).
5. Khotanlou H. **2008**. 3D brain tumors and internal brain structures segmentation in MR images. Ph. D. thesis in signal and images ,ENST, Paris Tech.
6. Florent Ségonne, **2002**. Unsupervised Skull Stripping in MRI. Master thesis (M.Sc.) in Electrical Engineering and Computer Science. Massachussets Institute of Technology.

7. Smitha S., Kumaran N., and Revathy K . **2009**. Quantitative analysis of brain tissues from Magnetic Resonance images. International Conference on Digital Image Processing, IEEE, DOI 10.1109/ ICDIP. 34.

8. Maragos P. and Schafer R. W. **1987**. Morphological Filters-Part I: Their Set Theoretic Analysis and Relations to Linear Shift –Invariant Filters. *IEEE Transactions on Acoustic, Speech, Signal Processing*. 35. pp: 1153-1169.

9. Swati T., Ashish B. and Rupali S. **2012**. Identification of Brain Tumors in 2D MRI using Automatic Seeded Region Growing Method. *Journal of Education*. 2(1). pp: 41-43.

10. Gonzalez R.C. and Woods R.E., **2002**. *Digital Image Processing*. Prentice Hall.

11. Gonzalez R.C, Woods R.E and Eddins S.L. **2004**. *Digital Image Processing Using MATLAB*. Pearson Prentice-Hall.

12. Asma'a A. A. Al-Tamimy**. 2005**. Artificial Intelligence for MagneticResonence Image (MRI) Recognition. M.Sc. Thesis in Medical Engineering, University of ALNAHRAIN, Iraq.

13. Serra J. **1982**. *Image Analysis and Mathematical Morphology*. Academic Press, New York.

14. Blake, A. and Isard, M. **1998**. *Active Contours*. Springer, London – UK.

15. Kass M., Witkin A., and Terzopoulos D. **1987**. Snakes: Active Contour models, Proceedings of First International Conference on Computer Vision, London. 1(4). pp: 259-269.

16. Atkins M.S., Mackiewich B.T. **1998**. Fully automatic segmentation of the brain in MRI. *IEEE Trans. Med. Imag*. 17. pp: 98–107.

17. Davatzikos C.A., Prince J.L. **1995**. An active contour model for mapping the cortex. *IEEE Trans. Med. Imag*. 14 (1), pp: 65–80.

18. Duta N, Sonka M. **1998**. Segmentation and interpretation of MR brain images: An improved active shape model. *IEEE Trans. Med. Imag*. 17(6). pp: 1049-1062.

19. Caro A., Rodríguez P. G., Cernadas E., Durán M. L. and Antequera T. **2003**. Potential Fields as an External Force and Algorithmic Improvements in Deformable Models. *Electronic Letters on Computer Vision and Image Analysis*. 2(1). pp: .25-36.

20. Ranganath, S.**1995**. Contour Extraction from Cardiac MRI Studies Using Snakes. *IEEE Transactions on Medical Imaging*. 14. pp: 328-338.

21. Caro, A., Rodríguez, P. G., Cernadas, E., Durán, M. L., Muriel, E., and Villa, D. **2001**. Computer Vision Techniques Applying Active Contours to Muscle Recognition in Iberian Ham MRI. Proc. International Conference on Signal Processing, Pattern Recognition and Applications 1, pp:62-66.

22. Chen C.W., Luo J., and Parker K. J. **1998**. Image segmentation via adaptive K-mean clustering and knowledge-based morphological operations with biomedical applications. *IEEE Trans. on Medical Imaging*. vol. 7. pp: 1673–1683.

23. Sueli A. M. and Joab O. L. **2006**. Comparison SOM Neural Network with Fuzzy C-Means, K-Means and Traditional Hierarchical Clustering Algorithms. *European Journal of Operational Research.* 17. pp: 1742-1759.

24. Yong Y. and Shuying H. **2007**. Image Segmentation By Fuzzy C- Means Clustering Algorithm With A Novel Penalty Term. *Computing and Informatics*. 26. pp : 17-31.

25. Zhang D. Q., Chen S. C., Pan Z. S. and Tan K. R. **2003**. Kernel- Based Fuzzy Clustering Incorporating Spatial Constraints for Image Segmentation. Proc. International Conference on Machine Learning and Cybernetics. Vol. 4. pp: 2189-2192.

26. Bezdec J.C. **1981**. *Pattern Recognition with Fuzzy Objective Function Algorithms*. Plenum Press, New York.

27. Chang Y.L., Li X. **1994**, Adaptive Image Region-Growing. *IEEE Trans. on Image Processing*. 3(6). pp: 868-872.

28. Adams R. and Bischof L. **1994**. Seeded region growing. *IEEE Transaction on Pattern Analysis and Machine Intelligence*. 16(6). pp: 641-647.

29. Alan W. L. and Hong Y. **2006**. Current Methods in the Automtaic Tissue Segmentation of 3D Magnetic Resonance Brain Images. Current Medical Imaging Reviews. 2(1).

30. Xuad J., Tulay A. and Wang Y.**1995**. Segmentation of Magnetic Resonance Brain Image: Integrating Region Growing and Edge Detection. *IEEE*. pp: 544-547.

31. Ali S.M., Loay K. A. and Rabab S. A. **2013**. Brain Tumor Extraction in MRI images using Clustering and Morphological Operations Techniques. *International Journal of Geographical Information System Applications and Remote Sensing*. 4(1). pp: 12-25.